Eurasian Journal of Analytical Chemistry
ISSN: 1306-3057 OPEN ACCESS 2018 13 (3): 1090-1100

Smart Detection of Blockage in Coronary Artery in Angiography

M. Ramamoorthy, N. Ayyanathan, M. Padma Usha

Received: 22 Jan 2018 ▪ Revised: 27 March 2018 ▪ Accepted: 20 April 2018

Abstract: In computer aided diagnosis of artery motion analysis coronary angiogram segmentation is of crucial importance. With vascular structures along with considerable variation in intensities and noise it is challenging to develop an automated and accurate vessel segmentation algorithm. The proposed approach is an unsupervised approach with coronary angiography as the source and is used to extract the vascular centerlines and segment the vessels and detect the blockages in the coronary artery. Initially a preprocessing step is applied to enhance and remove the low frequency noise in the image based on a contrast limited adaptive histogram equalization and morphological filters. The vascular structure is extracted by using Morphological hessian based approach and region based Otsu thresholding. Two different scales are used to extract the wide and thin vessels. Then the vessel centerline is extracted. A branch detection algorithm is employed to find the bifurcation. The blockages are detected by considering the diameter along the cross sectional area of the vessel. The proposed system has been analyzed and the experimental results conducted on several images prove the efficiency of the proposed method producing an accuracy of 96.98%.

Keywords: Coronary Artery, Vessel Extraction, Centerline Extraction, Morphological Operation, Thresholding, Histogram Equalization.

INTRODUCTION

Blockages in the arteries of the heart lead to Coronary artery disease (CAD) which is mainly due to the deposition of plaque. This is the most fatal disease in the developed countries causing a death rate of one third to one half in persons in the age limit of 35 to 64. In spite of the early successful detection techniques available, prior to heart attacks only 20% of the coronary artery diseases are diagnosed. Vascular structures vary in image intensities and noise as well as have varying cross sections and hence developing a fully automatic and accurate vessel segmentation algorithm is highly challenging. Extraction of vessel from coronary angiography images using intensity information is insufficient as the contrast variation along the vessels and intensity ambiguities can cause leakages. Usage of shapes prior to vessel segmentation is also challenging as the diseased vessel have abnormal and different shapes.

Several methods have been proposed for the automatic segmentation of vascular structures. One such segmentation method adopts a boundary model to extract the boundaries in the segmented image based on intensity or gradient information. From the training data available the boundary model is constructed [1-2]. A vessel extraction techniques based on parametric curve evolution is reviewed in [3]. The centerline is extracted is pioneered in [4]. In [5] at the vessel branch the user inputs have to be provided. In this the author models the vessel structure as a envelope of collection of spheres, thus providing a tubular vessel model. The background and the vessel intensity distribution are estimated based on the intensity histogram which is used to push the level set to capture the vessel boundaries. The segmentation is based on minimal path technique. A level set method based on the information from histogram is used to deform the initialized vessel which is obtained from the registration of pre segmented reference image [6].

M. Ramamoorthy, Assistant Professor, Department of Computer Science and Engineering, BIST, BIHER, Bharath Institute of Higher Education & Research, Selaiyur, Chennai. E-mail: saimoorthy123@gmail.com

N. Ayyanathan, Associate Professor, Master of Computer Applications, B.S. Abdur Rahman Crescent Institute of Science & Technology, Chennai, India. E-mail: n.ayyanathan@crescent.education

M. Padma Usha, Assistant Professor, Electronics and Communication Engineering, B.S. Abdur Rahman Crescent Institute of Science & Technology, Chennai, India. E-mail: padmausha@crescent.education

The new variational approach of segmentation based on level set approach under intensity in homogeneity is discussed in [7]. In [8] the vessel and its branches are detected based on the model of each vessel as a tubular structure without requiring end points of the vessel. Another method for extraction coronary artery is discussed in [9]. In this method an adaptive and multi-hierarchy method is used to preprocess the angiographic image. Sub images are obtained at different levels are fused to obtain the final image. A matched filter based techniques is adapted to enhance and segment the retinal vessels with double sided thresholding and first order derivative of Gaussian image [10]. In [11] morphological filters are used to enhance the vessels. Generally, vessel segmentation methods can be classified as supervised and unsupervised classifications. Supervised method of segmenting vessels is discussed in [12] and unsupervised technique is discussed in [13]. Yet another method is proposed to extract the cardiac vascular structure using multiscalemedialness function [14]. In this method, the blood vessels are extracted and the 3D structure of the vascular structure is reconstructed by using volume rendering technique.

The proposed system is used to segment the vascular structure in the coronary angiography images and to detect the blockages. The paper is organized as follows: Section II describes the preprocessing step. Further the centerline is extracted and vessel branching algorithm is used to find the bifurcation. Finally the blockages in the vessels are identified. Section III discusses the performance evaluation of the proposed method with the methods described in [9] and [14]. Finally Section IV concludes the proposed method.

PROPOSED METHOD

The proposed technique is an integrated structure designed to solve the problem of segmentation of coronary angiogram. First the image is enhanced and it walks across the intensity gaps along the vessel direction and extract the vessel bifurcations. The flow chart of the proposed method is shown in fig 1.

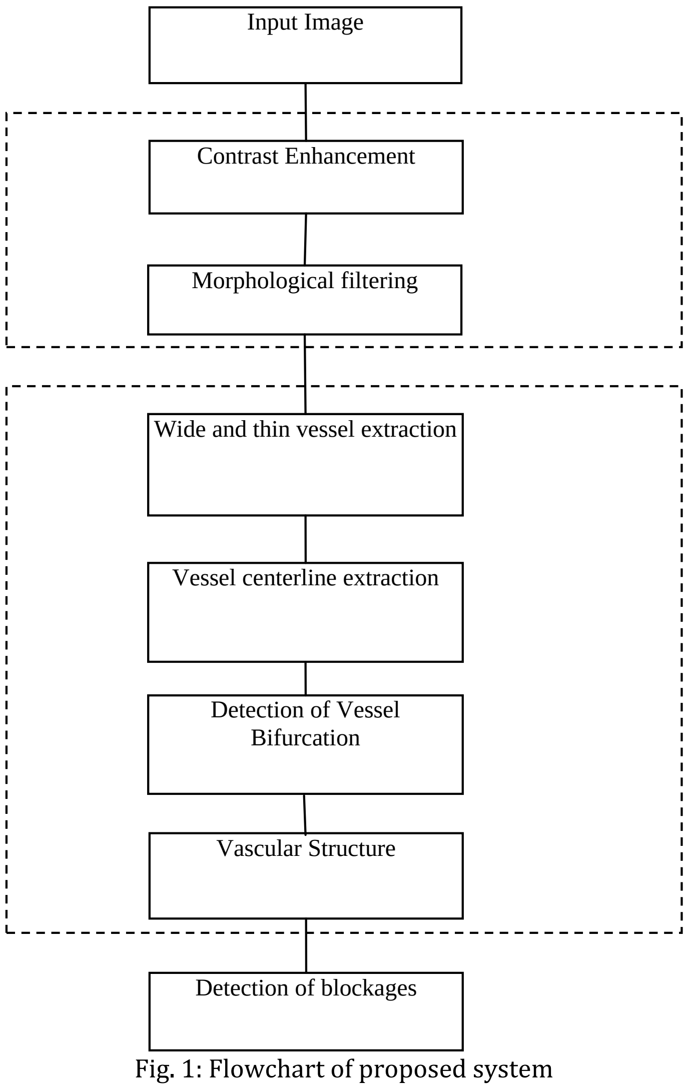

Fig. 1: Flowchart of proposed system

A. Preprocessing

The first step is the preprocessing which is used to enhance the image and perform illumination corrections on the source image.

A.1) Contrast Limited Adaptive Histogram Equalization

Contrast limited adaptive histogram equalization is performed to enhance the image. Histogram equalization is done by stretching the gray level values of low contrast image [15]. In this method the image is divided into regions and local histogram equalization is performed [16]. The clip value is user defined. The noise level to be smoothened and the contrast level to be enhanced can be specified in the clipping limit. In this paper, the clipping limit is chosen from 0 to 0.01.

A.2) Morphological Filtering

The vascular structures are enhanced using morphological filters. Vascular structures appear more contrast than the back ground. This change is reflected adversely in the entire process of vessel extraction. The morphological filter is based on top hat transform. The width of the widest vessel set as reference. In the proposed technique the width of the vessel varies between 1 to 8 pixels. The top hat transformation is sensitive to noise. It causes the pixel values in the opened image to be less than or equal to the pixel values in the input image. This leads to intensity variation. To overcome the issue a modified top hat transform [11] is proposed which perform a closing operation followed by opening operation without using any comparator or minimal operator. In this paper, the structure element is chosen as disk type with radius 8 pixels. Equation (1) through (3) defines the various top hat operations.

The opening top hat transform in an image I with S as the structure element is defined as:

$$T_{open}=I \text{ o } S_o \tag{1}$$

The closing top hat transform in an image I with S as the structure element is defined as:

$$T_{close}=I .S_c \tag{2}$$

The modified top-hat transform, T is defined as:

$$T=1-(I.S_c) \text{ o } S_o \tag{3}$$

B. Extracting Wide and Thin Vessels

The hessian matrix and Eigen value approach are used to extract the wide and thin vessels from the morphological enhanced image and the vascular structures are extracted using Otsu thresholding. The second order derivative at different scales is used to represent the vessels with variable width. Suppression of non vascular structure and contrast enhancement is done using the difference in the eigen values of hessian matrix.

The hessian matrix on a directional image I_i, in a coordinate x'y' is defined as:

$$H = \begin{bmatrix} h_{11} & h_{12} \\ h_{21} & h22 \end{bmatrix} \tag{4}$$

Where

$$h_{11} = \frac{\partial^2 I_i}{\partial x^2}\cos^2\theta_i + \frac{\partial^2 I_i}{\partial x \partial y}\sin(2\theta_i) + \frac{\partial^2 I_i}{\partial y^2}\sin^2\theta_i \tag{5}$$

$$h_{22} = \frac{\partial^2 I_i}{\partial x^2}\sin^2\theta_i - \frac{\partial^2 I_i}{\partial x \partial y}\sin(2\theta_i) + \frac{\partial^2 I_i}{\partial y^2}\cos^2\theta_i \tag{6}$$

$$h_{12} = h_{21} = -\frac{1}{2}\frac{\partial^2 I_i}{\partial x^2}\sin(2\theta_i) - \frac{\partial^2 I_i}{\partial x \partial y}\cos(2\theta_i) + \frac{1}{2}\frac{\partial^2 I_i}{\partial y^2}\sin(2\theta_i) \tag{7}$$

The eigen values λ_1 and λ_2 are obtained as follows.

$$h'_{11} = \sigma^2 * h_{11} \tag{8}$$

$$h'_{22} = \sigma^2 * h_{22} \tag{9}$$

$$h'_{21} = h'_{12} = \sigma^2 * h_{21} \tag{10}$$

$$[\lambda_1 \lambda_2] = eigen2img(h'_{11}, h'_{12}, h'_{22}) \tag{11}$$

Where, σ defines the scales for vessel enhancement. The computational complexity is reduced [17] by taking the difference image $I = \lambda_2 - \lambda_1$. In this paper, σ is chosen as 1 and 2.5.

C) Centerline Extraction

Vessels are anatomical structures that provide large information for localization of features. Several techniques have been proposed for vessel centerline extraction based on hessian method, gabor filter, matched filter and edge based methods. In this paper a matched filter is applied to extract the centerline in the vascular structure. Gaussian functions are used as kernel in matched filters. However, the intensity of some wide vessels is not Gaussian, then Gaussian-Hermite mixture model is used to extract the centerline[18]. To detect vessel in any direction, the two dimensional kernel is represented as two one dimensional kernels. Let the image intensity at the position (u,v) be represented as I(u,v). Then the matched filter response R in the orientation θ is given as:

$$R(u,v,\theta) = -\int\int_{-\infty}^{\infty} H_{vv}(v-x)H(u-y)I(x,y,\theta)dxdy \tag{12}$$

Where H(x) represent the Gaussian Hermite kernel in the normal direction and the 1D second order kernel is defined as:

$$H(x) = (1 + a(x^2 - 1))\frac{1}{2\pi\sigma^2}e(-x/2\sigma^2) \tag{13}$$

Finally, the centerline is extracted by maximizing the response of overall orientation of each pixel.

D) Detection of Vessel Bifurcation

The vascular structure grows out and then constructs new branches. The challenge is to detect the vessel branches. An algorithm is proposed to detect the vessel branches as it moves through the vessel tree.

Algorithm:

1. Construct a sphere S^2 of radius R.
2. Sample N directions d_i.
3. Construct the tubes of radius 1 and length R along each N directions.
4. Estimate the mean intensity in each tubes as $I_{mean}(d_i)$.
5. Apply threshold to the estimated intensity with respect to the parent intensity I_{thres}.
6. Apply the subset of directions d_i with the mean intensities above the threshold.
1. To the extracted direction apply k-means clustering[19]. That That is $d_i \forall i \in (1, N)$ and $I_{mean}(d_i) \geq I_{thres}$ with three clusters[20].
7. If number of clusters less than 3 then
   No branches
8. Else
   i) Compute the centroid of the direction in each cluster. This results in 3 branch directions.
   ii) The direction that has the maximum overlap compared to the parent branch volume is eliminated.
   iii) Perform dot product of remaining directions with the tangent of parent branch at the end point.
   iv) The parent branch is extended by the candidate direction that is better aligned with the tangent at the end point.
   v) A new branch is created using the remaining candidate direction in the tree structure.

E) Detection of Blockages

The detection of blockage in the blood vessel and quantification is done based on the cross sectional area A_i of the vessel computed along the centerline at each position i. The value of i ranges between 1 to n, where n represent the number of positions in the centerline. Then the radius is defined as:

$$R = \sqrt{\frac{A_i}{\pi}} \tag{14}$$

Calculate the diameter of the D. Detection of blockages are done as follows:

i) Let D_{i-1} be the diameter at position P_{i-1}

ii) $D_{i,n-1}=D_{i-1}$

iii) If $(D_{i,n}>D_{i,n-1})$ then

a. The positions with $D_{i,n}$is less than the diameter centered at $P_{i,n-1}$ is computed.

b. The positions calculated above are detected as blockages.

From the extracted vessel tree the blockage in the artery are detected and is shown in figure 2.

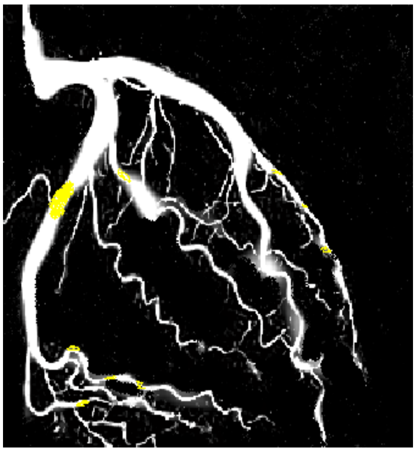

Fig. 2: Blockage detected are marked in yellow color

RESULTS AND DISCUSSION

The proposed algorithm is tested on real image with blockages. The proposed algorithm is implemented in Matlab 12 on i3 processor.

To adjust some parameters the algorithm is tested in simulated images and to obtain the actual performance the proposed method is evaluated in actual images. The proposed method has several characteristics: i) it is powerful to the detected starting point. ii) it can track along the vessel tree without any user interaction. ii) it can automatically detect blockages by considering the narrowing of blood vessels based on the diameter. The computational time in preprocessing is very minor about 8s, the time to track the vessels and centreline is about 20s and the time to detection blockages is about 12s. Even though the coronary artery is segmented automatically, still there is a room for detection of blockages. Blockages are detected based on the diameter profile and long blockages remain underestimated. In the proposed method long blockages are considered based on the minimal diameter in the narrowing artery. The detailed experimental results are shown in fig 3&4. The proposed method dealt with minimum false positives. On an average 23false positives in 15 datasets.

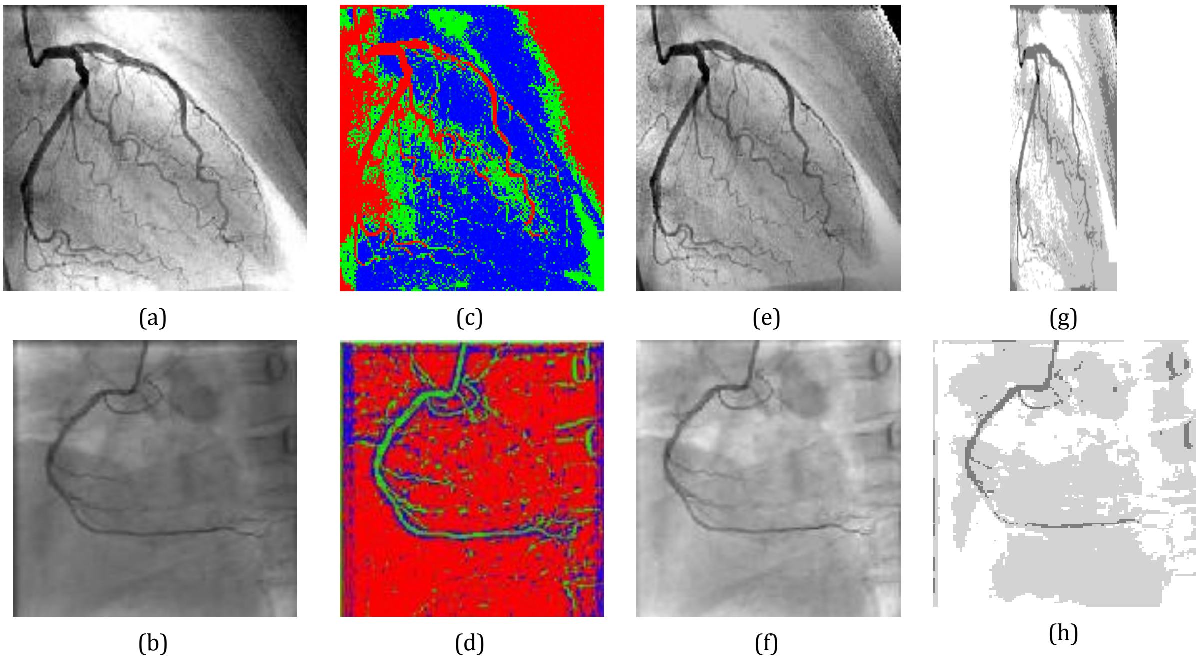

Fig. 3: Preprocessed Image (a)-(b) Input image (c)-(d)partitioned with local regions (e)- (f) Contrast limited Histogram equalization (g) – (h) Morphological Filtering

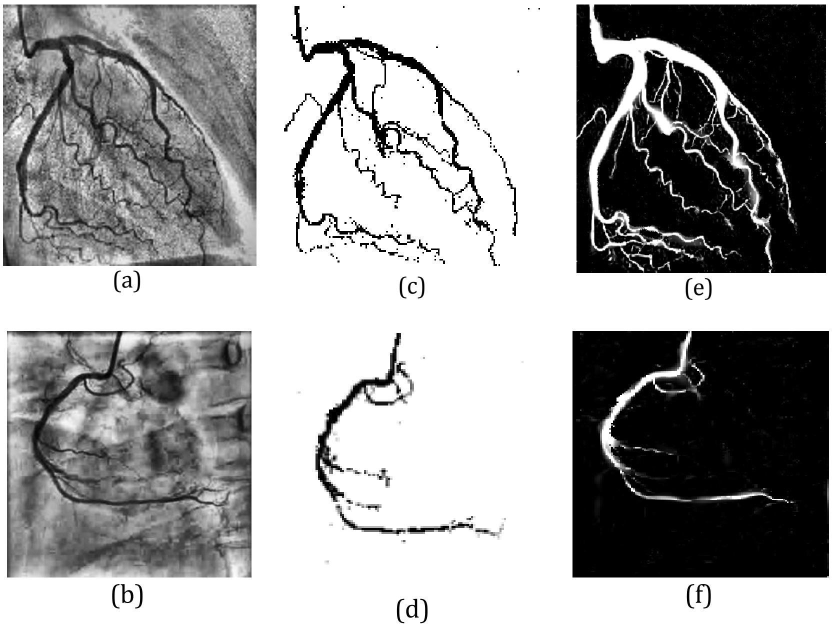

Fig. 4: Extracted Vessel Structure (a)-(b) Vessels enhanced (c)-(d) Segmented thin and thick vessels (e)-(f) Extracted vascular structure in binary

Several performance metrics are used to evaluate the performance of the proposed method. Equations (15) - (18) quantify the proposed system with manual segmentation. Percentage of overlapped vessel pixels that is, True positive (TP) are used to find the Sensitivity of the proposed method.

$$Sensitivity = \frac{No.OfOverlappedVesselpixels}{TotalNoOfVesselPixelsInManualSegmentation} x100 \qquad (15)$$

Specificity is evaluated based on false positive (FP) rate. False positive is the number of pixels available in automatic segmentation but not in manual segmentation among the total pixels present in automatic segmentation. In exceptional cases, the specificity would be useful to detect the true contours missed in manual segmentation.

$$Specificity = 1 - \frac{No.OfVesselpixelsInAutomaticSegmentation, butNotInManual}{TotalNoOfVesselpixelsInAutomaticSegmentation} x100 \qquad (16)$$

Table 1 shows the performance of the posed system in terms of sensitivity and specificity. The F1 measure is evaluated based on true negative(TN) values. That is the percentage of pixels available in manual segmentation but not present in automatic segmentation among the total number of pixels present in manual and automatic segmentation.

$$F1measure = 1 - \frac{No.OfVesselpixelsInManual, butNotInAutomaticSegmentation}{TotalNoOfVesselpixelsInManualandAutomaticSegmentation} x100 \qquad (17)$$

Accuracy is used to measure the no of pixels in vessels segmented in automatic segmentation.

$$Accuracy = \frac{TruePositive + TrueNegative}{TruePositive + TrueNegative + FalsePositive} x100 \qquad (18)$$

The segmentation of coronary artery and detection of blockages can assist clinicians to a great extent in making diagnosis of coronary artery diseases. Accurate diagnosis of coronary diseases can be obtained by isolating the vessels from other irrelevant anatomical structures and by visualizing the coronary tree from the proximal end to distal end. The proposed algorithm was tested on 15 patient datasets. The results of performance evaluation on 6 dataset are shown in table 1.

Table 1: Comparison of Performance metrics

Data Set	Proposed			Work [9]			Work [14]		
	Sensitivity	Specificity	F1 measure	Sensitivity	Specificity	F1 measure	Sensitivity	Specificity	F1 measure
1	99.08	93.33	99.55	96.92	98.44	98.45	88.62	94.43	94.13
2	98.8	94.28	99.41	93.15	95.94	96.52	96.52	88.78	98.33
3	84.41	96.47	91.69	76.47	87.39	87.45	59.12	73.63	77.32
4	95.61	87.55	97.9	96.05	87.95	98.11	72.81	86.01	85.27
5	98.25	99.62	99.12	93.86	95.54	96.9	93.86	95.17	96.91
6	93.75	99.75	96.78	95.14	96.71	97.55	90.05	97.74	94.82

The proposed algorithm is developed in order to attain an optimal performance, with an average sensitivity of 96.08%, average specificity of 2.93% and an average F1 measure of 1.33%. Figure 5 and Figure 6 shows the comparative performance measures of the proposed work.Based on the locations of discrepancies, in some cases further adjustments may not be required, given that the discrepancy may not be directly related to any segment of the vessels. As the segmentation approaches the distal end in the vessel, the sensitivity tends to decrease in the proposed algorithm.

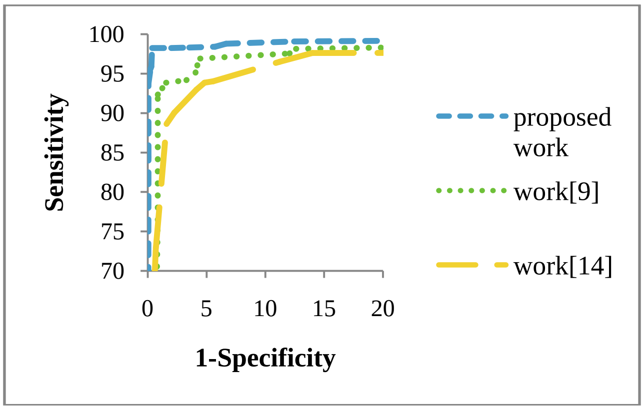

Fig. 5: Analysis of Sensitivity and 1-specificity

To evaluate the performance of the proposed system against the manual segmentation, two more performance metrics[21] are used: Area Overlap (AO) and False Discovery Rate (FDR). The metrics are calculated as follows:

$$AO = \frac{P_1 \cap P_2}{P_1} \tag{19}$$

whereP_1 represents the segmented vessel pixel obtained by the proposed algorithm and P_2 represents the vessel pixel in manual segmentation.

Finally, the False Discovery rate is calculated.

$$FDR = \frac{FalsePositive}{TruePositive + FalsePositive} \tag{20}$$

Where True Positive represents correctly identified vessel pixel, False Positive represents incorrectly identified vessel pixel, True Negative represents correctly rejected vessel pixel. Table 2 shows the performance assessment of the proposed work on a sample of 6 datasets. From the results, it is clear that the proposed method offers better results for vessel segmentation.

Table 2: Shows the performance assessment of proposed approach

Dataset	Accuracy	Area Overlap	False Discovery Rate
1	93.39	93.33	6.67
2	94.35	94.28	5.72
3	97	96.47	3.53
4	88.03	87.55	12.45
5	99.63	99.62	0.38
6	99.77	99.75	0.25

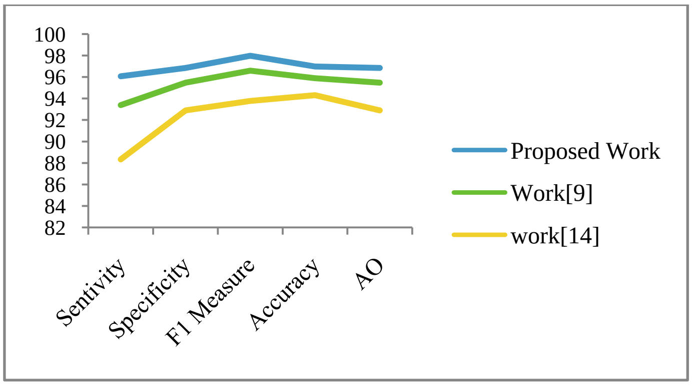

Fig. 6: Performance analysis of various measures

Performance assessment is evaluated using equation (21) – (23) on 22 dataset and the work is compared with the algorithm implemented earlier by Jiji G.W [14] and Qingzhu Wang et.al[9]. The results of evaluation are given in Table 3. The results show that the proposed method outperforms the earlier works which is precise by the average of false positive rate and false discovery rate. To evaluate the detection of vessel segments the Percentage of detected artery segment (DAS) is calculated. Detectedartery segment (DAS) produced by [9] reached 95.46% and DAS% produced by [14] is 92.36% and the proposed method produced 97%.

Table 3: Performance evaluation: Comparison between the proposed algorithm and work done in [9] and [14]

Methods	Accuracy	Area Overlap	False Discovery Rate
Proposed Work	96.98	96.855	3.145
Work [9]	95.899	95.48	4.52
Work [14]	94.32	92.905	7.095

The limitation of the proposed work is that the centerline extraction step requires initialization of start point of coronary artery. For each data set the user has to interpret the start point. After initialization the centerlines can be automatically obtained in the vessels and across vessel branches. Blockages can be detected with the centerlines.

CONCLUSION

The proposed method allows for segmentation of vessels and detection of blockages in the coronary artery. The experimental results show that the proposed method produced results with similar precision to that of experts. The results showed that the average sensitivity overall 15 data set is 96.08% with a standard deviation of $\pm$ 3.95. In future the work is to be extended in detection of blockages by integrating the morphological and intensity features which may lead to improvements in better detection of blockages and also to estimate the percentage of blockage.

REFERENCES

[1] Udayakumar, R., Khanaa, V., & Saravanan, T. (2013). Analysis of polarization mode dispersion in fibers and its mitigation using an optical compensation technique. *Indian Journal of Science and Technology*, *6*(6), 4767-4771.

[2] Yan, S., Gao, M., Qi, B., & Jiang, X. (2014). Blast Wave Propagation and Casualty Distribution Evaluation in the Subway Station Subjected to Internal Blast Loading. *The SIJ Transactions on Advances in Space Research & Earth Exploration, 2*(1), 6-11.

[3] Geetha, K., Preethy, C., and Thenmozhi, P. (2017). Simulation Model of Solar Induction Motor Drive System Using SVPWM Technique. *Bonfring International Journal of Power Systems and* Integrated *Circuits, 7*(1), 1-6.

[4] Archana Lal, P. (2014). A Neural Network Based Analysis of Altered Fingerprints. International Scientific *Journal on Science Engineering & Technology*, *17*(9), 863-868.

[5] AlaguPandian, P., Sakthivel, K., Sheik Alavudeen, K., & R.LakshmiPriya. R. (2017). A Low Power Efficient Design of Full Adder Using Transmission Gate. *International Journal of Communication and Computer Technologies, 5*(1), 1-5.

[6] SakthiPriya V., & Vijayan, M., (2017). Automatic Street Light Control System Using WSN Based on Vehicle Movement and Atmospheric Condition. *International Journal of Communication and Computer Technologies, 5*(1), 6-11.

[7] Sowmiya, E., Dr.Chandrasekaran, V., & Sathya, T. (2017). Sensor Node Failure Detection Using Round Trip Delay in Wireless Sensor Network. *International Journal of Communication and Computer Technologies, 5*(1), 12-16.

[8] Senthil Kumar, B., & Dr.Srivatsa, S.K.(2014). Opportunistic Channel Access Algorithm Based on Hidden Semi Markov Model for Cognitive Radio Networks. *Bonfring International Journal of* Research *in Communication Engineering, 4*(2), 17-21.

[9] Angeline, D.M.D., (2013). Association Rule Generation for Student Performance Analysis using Apriori Algorithm. *The SIJ Transactions on Advances in Space Research & Earth Exploration, 1*(1), 16-20.

[10] Preethi, L., & Dr.Periyasamy, S. (2018). Enhanced Scalable Learning for Identifying and Ranking for Big Data Using Social Media Factors. *Bonfring International Journal of Software Engineering and Soft Computing, 8*(1), 31-35.

[11] Saikong, W., & Kulworawanichpong, T. (2014).Voltage Stability Assessment in DC Railways with Minimum Headway Consideration. *The SIJ Transactions on Computer Networks & Communication Engineering (CNCE), 2*(4), 1-6.

[12] Udayakumar, R., Kumaravel, A., & Rangarajan, K. (2013). Introducing an efficient programming paradigm for object-oriented distributed systems. *Indian Journal of Science and Technology*, *6*(5S), 4596-4603.

[13] Mageswaran, S.U., & Sekhar, N.G. (2013). Reactive power contribution of multiple STATCOM using particle swarm optimization. *International Journal of Engineering & Technology*, *5*(1), 122-126.

[14] Giri, R.K., & Saikia, M. (2013). Multipath routing for admission control and load balancing in wireless mesh networks. *International Review on Computers and Software*, *8*(3), 779-785.

[15] Padmapriya, G., Manikandan, A., Krishnasamy, V., Jaganathan, S.K., & Antony, S.A. (2016). Spinel NixZn1− xFe2O4 (0.0≤ x≤ 1.0) nano-photocatalysts: synthesis, characterization and photocatalytic degradation of methylene blue dye. *Journal of Molecular Structure*, *1119*, 39-47.

[16] Vijayaragavan, S.P., Karthik, B., Kiran Kumar, T.V.U., & Sundar Raj, M. (2013). Analysis of chaotic DC-DC converter using wavelet transform. *Middle-East Journal of Scientific Research*, *16*(12), 1813-1819.

[17] Lokesh, K., Kavitha, G., Manikandan, E., Mani, G.K., Kaviyarasu, K., Rayappan, J.B.B., ... & Maaza, M. (2016). Effective ammonia detection using n-ZnO/p-NiO heterostructured nanofibers. *IEEE Sensors Journal*, *16*(8), 2477-2483.

[18] Abraham, A.G., Manikandan, A., Manikandan, E., Vadivel, S., Jaganathan, S.K., Baykal, A., & Renganathan, P.S. (2018). Enhanced magneto-optical and photo-catalytic properties of transition metal cobalt (Co2+ ions) doped spinel MgFe2O4 ferrite nanocomposites. *Journal of Magnetism and Magnetic Materials*, *452*, 380-388.

[19] Kennedy, J., Fang, F., Futter, J., Leveneur, J., Murmu, P.P., Panin, G.N., & Manikandan, E. (2017). Synthesis and enhanced field emission of zinc oxide incorporated carbon nanotubes. *Diamond and Related Materials*, *71*, 79-84.

[20] Teresita, V.M., Manikandan, A., Josephine, B.A., Sujatha, S., & Antony, S.A. (2016). Electromagnetic properties and humidity-sensing studies of magnetically recoverable LaMg x Fe 1− x O 3− δ perovskites nano-photocatalysts by sol-gel route. *Journal of Superconductivity and Novel Magnetism*, *29*(6), 1691-1701.

[21] Caroline, M.L., & Vasudevan, S. (2009). Growth and characterization of pure and doped bis thiourea zinc acetate: Semiorganic nonlinear optical single crystals. *Current applied physics*, *9*(5), 1054-1061.

[22] Jayalakshmi, V., & Gunasekar, N.O. (2013). Implementation of discrete PWM control scheme on Dynamic Voltage Restorer for the mitigation of voltage sag/swell. *International Conference on Energy Efficient Technologies for Sustainability*, 1036-1040.

[23] Udayakumar, R., Khanaa, V., & Kaliyamurthie, K.P. (2013). Optical ring architecture performance evaluation using ordinary receiver. *Indian Journal of Science and Technology*, *6*(6), 4742-4747.

[24] Udayakumar, R., Khanaa, V., & Kaliyamurthie, K.P. (2013). Performance analysis of resilient ftth architecture with protection mechanism. *Indian Journal of Science and Technology*, *6*(6), 4737-4741.

[25] Saravanan, T., Srinivasan, V., & Sandiya, V.P. (2013). A two stage DC-DC converter with isolation for renewable energy applications. *Indian Journal of Science and Technology*, *6*(6), 4824-4830.

[26] Sundarraj, M. (2013). Study of compact ventilator. *Middle-East Journal of Scientific Research*, *16*(12), 1741-1743.

[27] Thema, F.T., Manikandan, E., Gurib-Fakim, A., & Maaza, M. (2016). Single phase Bunsenite NiO nanoparticles green synthesis by Agathosma betulina natural extract. *Journal of alloys and compounds*, *657*, 655-661.

[28] Sathyaseelan, B., Manikandan, E., Sivakumar, K., Kennedy, J., & Maaza, M. (2015). Enhanced visible photoluminescent and structural properties of ZnO/KIT-6 nanoporous materials for white light emitting diode (w-LED) application. *Journal of Alloys and Compounds*, *651*, 479-482.

[29] Gopalakrishnan, K., Prem Jeya Kumar, M., Sundeep Aanand, J., & Udayakumar, R. (2013). Analysis of static and dynamic load on hydrostatic bearing with variable viscosity and pressure. *Indian Journal of Science and Technology,* 6(6), 4783-4788.

[30] Prabhu, M.R., Reji, V., & Sivabalan, A. (2012). Improved radiation and bandwidth of triangular and star patch antenna. *Research Journal of Applied Sciences, Engineering and Technology*, *4*(12), 1740-1747.

[31] Arumugam, S. and Ramareddy, S. (2012). Simulation comparison of class D/ Class E inverter fed induction heating. *Journal of Electrical Engineering*, 12(2), 71-76.

[32] Udayakumar, R., Khanaa, V., & Kaliyamurthie, K.P. (2013). High data rate for coherent optical wired communication using DSP. *Indian Journal of Science and Technology*, *6*(6), 4772-4776.

[33] Nagarajan, C., & Madheswaran, M. (2012). Experimental Study and Steady State Stability Analysis of CLL-T Series Parallel Resonant Converter with Fuzzy Controller using State Space Analysis. *Iranian Journal of Electrical and Electronic Engineering*, *8*(3): 259-267.

[34] Gopalakrishnan, K., PremJeya Kumar, M., SundeepAanand, J., & Udayakumar, R. (2013). Thermal properties of doped azopolyester and its application. *Indian Journal of Science and Technology*, *6*(6), 4722-4725.

[35] Kumaravel A., Meetei O.N. (2013). An application of non-uniform cellular automata for efficient cryptography. *Indian Journal of Science and Technology*, *6*(5): 4560-4566.

[36] Kumaravel, A., & Pradeepa, R. (2013). Layered approach for predicting protein subcellular localization in yeast microarray data. *Indian Journal of Science and Technology*, *6*(5S), 4567-4571.

[37] Kaviyarasu, K., Manikandan, E., Kennedy, J., & Maaza, M. (2016). Synthesis and analytical applications of photoluminescent carbon nanosheet by exfoliation of graphite oxide without purification. *Journal of Materials Science: Materials in Electronics*, *27*(12), 13080-13085.

[38] Mathubala, G., Manikandan, A., Antony, S.A., & Ramar, P. (2016). Photocatalytic degradation of methylene blue dye and magneto-optical studies of magnetically recyclable spinel NixMn1-xFe2O4 (x= 0.0–1.0) nanoparticles. *Journal of Molecular Structure*, *1113*, 79-87.

[39] Manikandan, E., Kennedy, J., Kavitha, G., Kaviyarasu, K., Maaza, M., Panigrahi, B.K., & Mudali, U.K. (2015). Hybrid nanostructured thin-films by PLD for enhanced field emission performance for radiation micro-nano dosimetry applications. *Journal of Alloys and Compounds*, *647*, 141-145.

[40] Kumaravel, A., & Meetei, O.N. (2013). An application of non-uniform cellular automata for efficient cryptography. *IEEE Conference on Information & Communication Technologies*: 1200-1205.

[41] Langeswaran, K., Gowthamkumar, S., Vijayaprakash, S., Revathy, R., & Balasubramanian, M.P. (2013). Influence of limonin on Wnt signalling molecule in HepG2 cell lines. *Journal of natural science, biology, and medicine*, *4*(1), 126-133.

[42] Srinivasan, V., & Saravanan, T. (2013). Analysis of harmonic at educational division using CA 8332. *Middle-East Journal of Scientific Research*, *16*(12), 1768-73.

[43] Josephine, B.A., Manikandan, A., Teresita, V.M., & Antony, S A. (2016). Fundamental study of LaMg x Cr 1− x O 3− δ perovskites nano-photocatalysts: sol-gel synthesis, characterization and humidity sensing. *Korean Journal of Chemical Engineering*, *33*(5), 1590-1598.

[44] Saravanan, T., Saritha, G., & Udayakumar, R. (2013). Robust H-Infinity Two Degree of Freedom Control for Electro Magnetic Suspension System. *Middle-East Journal of Scientific Research*, *18*(12), 1827-1831.

[45] Rajasulochana, P., Dhamotharan, R., Murugakoothan, P., Murugesan, S., & Krishnamoorthy, P. (2010). Biosynthesis and characterization of gold nanoparticles using the alga Kappaphycus alvarezii. *International Journal of Nanoscience*, *9*(05), 511-516.

[46] Slimani, Y., Güngüneş, H., Nawaz, M., Manikandan, A., El Sayed, H. S., Almessiere, M. A., & Baykal, A. (2018). Magneto-optical and microstructural properties of spinel cubic copper ferrites with Li-Al co-substitution. *Ceramics International*, *44*(12), 14242-14250.

[47] Kaviyarasu, K., Manikandan, E., Kennedy, J., Jayachandran, M., & Maaza, M. (2016). Rice husks as a sustainable source of high quality nanostructured silica for high performance Li-ion battery requital by sol-gel method–a review. *Adv. Mater. Lett*, *7*(9), 684-696.

[48] Ilayaraja, K., & Ambica, A. (2015). Spatial distribution of groundwater quality between injambakkamthiruvanmyiur areas, south east coast of India. *Nature Environment and Pollution Technology*, *14*(4), 771-776, 2015.

[49] Sharmila, S., Rebecca, L. J., Das, M.P., & Saduzzaman, M. (2012). Isolation and partial purification of protease from plant leaves. *Journal of Chemical and Pharmaceutical Research*, *4*(8), 3808-3812.

[50] Rajakumari, S.B., & Nalini, C. (2014). An efficient cost model for data storage with horizontal layout in the cloud. *Indian Journal of Science and Technology*, *7*(3), 45-46.